

Decomposition and Model Selection for Large Contingency Tables

Corinne Dahinden^{*1,2} and Peter Bühlmann^{1,2}

¹ Seminar für Statistik, ETH Zürich, CH-8092 Zürich, Switzerland

² Competence Center for Systems Physiology and Metabolic Diseases, ETH Zürich, CH-8093 Zürich, Switzerland

Received 2 April 2009

Summary

Large contingency tables summarizing categorical variables arise in many areas. For example in biology when a large number of biomarkers are cross-tabulated according to their discrete expression level. Interactions of the variables are generally studied with log-linear models and the structure of a log-linear model can be visually represented by a graph from which the conditional independence structure can then be read off. However, since the number of parameters in a saturated model grows exponentially in the number of variables, this generally comes with a heavy burden as far as computational power is concerned. If we restrict ourselves to models of lower order interactions or other sparse structures we face similar problems as the number of cells remains unchanged. This is in sharp contrast to high-dimensional regression or classification procedures because, besides a high-dimensional parameter, we have to deal with the analogue of a huge sample size. In addition, high-dimensional tables naturally feature a large number of sampling zeros which often leads to the nonexistence of the MLE estimate. We therefore present a divide-and-conquer approach, where we first divide the problem into several lower-dimensional problems and then combine these to form a global solution. Our methodology is computationally feasible for log-linear interaction modeling with many categorical variables each or some of them having many categories. We demonstrate the proposed method on simulated data and apply it to a bio-medical problem in cancer research.

Key words: Categorical Data, Graphical Model, Group Lasso, Log-Linear Models, Sparse Contingency Tables.

1 Background

We consider the problem of estimation and model selection in log-linear models for large contingency tables involving many categorical variables. This problem encompasses the estimation of the graphical model structure for categorical variables. This structure learning task for discrete graphical models has lately received considerable attention as it plays an important role in a broad range of applications and the resulting models can be used as probabilistic representation of the underlying distribution (Lauritzen, 1996). The conditional independence structure of the distribution can be read off directly from the graph and hence a graphical representation of the distribution is easy to understand. Graphical models for categorical variables correspond to a class of hierarchical log-linear interaction models for contingency tables. Thus, fitting a graph corresponds to model selection in a hierarchical log-linear model.

The difficulties concerning computational aspects can be ranked in the following increasing order. Graphical modeling for discrete categorical variables is easiest but it doesn't allow to infer the magnitude of the coefficients β in the log-linear model

$$\log(\mathbf{p}) = \mathbf{X}\beta,$$

* Corresponding author: e-mail: dahinden@stat.math.ethz.ch, Phone: +41 44 632 4276, Fax: +41 44 632 1228

see also formula (3). The next level of difficulty is the estimation of the unknown parameter vector β in a log-linear model whose full dimension equals the number of cells in the contingency table. For large tables, the dimension of β is huge but under some sparsity assumptions it is possible to accurately estimate such a high-dimensional vector using suitable regularization. The major problem is here that besides the high-dimensionality of β , the analogue of the sample size (the row-dimension of \mathbf{X}) is huge, e.g. 3^{40} for 40 categorical variables having 3 levels each. Finally, the most difficult problem is the estimation of the probability vector \mathbf{p} whose dimension equals again the number of cells in the table. It is rather unrealistic to place some sparsity assumptions on \mathbf{p} in the sense that many entries would equal exactly zero which would enable feasible computation. Therefore, it is impossible to ever compute an estimate of the whole probability vector \mathbf{p} (e.g. having dimensionality 3^{40}). Nevertheless, thanks to sparsity of the parameter vector β and the junction tree algorithm, it is possible to compute accurate estimates $\{\hat{\mathbf{p}}(i); i \in \mathcal{C}\}$ for any reasonable-sized collection \mathcal{C} of cells in the contingency table. Our presented methodology allows to do all these tasks for categorical variables having possibly different number of levels: inference of a graphical model for discrete variables, of a sparse parameter vector in a log-linear model and of a collection of cell probabilities. There is hardly any other method which can handle all these tasks for contingency tables involving many, say more than 20, variables. In Jackson *et al.* (2007) some dimensionality reduction is achieved by reducing the number of levels per variable. The reduction is accomplished by collapsing two categories by aggregating their counts if the two categories behave sufficiently similar. If d variables are considered, this method reduces the problem at best to d binary variables. For this special case with binary factors, an approach based on many logistic regressions can be used for fitting log-linear interaction models whose computational complexity is feasible even if the number of variables is large (Wainwright *et al.*, 2007). Another method to address the log-linear modeling problem for large contingency tables is proposed in Kim (2005) where the variables are grouped such that they are highly connected within groups but less between groups and graphical models are fitted for these subgroups. A graph-theoretical proof is given in Kim (2005) showing that the prime separators of the subgroups appear as prime separators of the full graph. The models are then combined using so-called graphs of prime separators. The implementation of the combination however is not an easy task and no exact algorithm is given on how to combine the models.

Motivated by the approach in Kim (2005), we also propose a so-called divide-and-conquer algorithm, where the dimensionality reduction is achieved by collapsing the table on certain variables and thereby reducing the problem to smaller tables which can be handled more easily. All the fitted lower-dimensional log-linear models are combined appropriately to represent an estimation of the joint distribution of all variables. The procedure enables us to handle very large tables e.g. up to hundreds of categorical variables, where some or all of them can have more than two categories. This multi-category framework cannot be treated by the approach in Wainwright *et al.* (2007) which can handle large binary tables only.

2 Preliminaries

We discuss here log-linear interaction models for contingency tables and establish the connection between the theory of graphical models and log-linear interaction models.

2.1 Log-Linear Interaction Model

We adopt here the notation of Darroch *et al.* (1980). Assume we have some factors or categorical variables, indexed by a set V . Each factor $v \in V$ has a number of levels I_v . The table is the set $I = \prod_{v \in V} I_v$. An individual cell is denoted by $i = (i_v, v \in V)$ and the corresponding cell count by n_i . For example, assume we have 2 binary variables, then $V = \{1, 2\}$, $I_1 = I_2 = \{0, 1\}$ and the individual cells are denoted by $(0, 0)$, $(0, 1)$, $(1, 0)$, $(1, 1)$. The total number of cells in a table is $m = |I| = \prod_{v \in V} |I_v|$, which equals 4 in our example. A natural way of representing the distribution of the cell counts is via a vector of probabilities $\mathbf{p} = (p(i), i \in I)$. In our example, this would correspond to defining probabilities for all four possible

combinations. If a total number of n individuals is observed which are classified independently, then the distribution of the corresponding cell counts $\mathbf{n} = (n_1, n_2, \dots, n_m)^t$ is multinomial with probability \mathbf{p} . The general log-linear interaction model specifies the unknown distribution \mathbf{p} as follows:

$$\log p(i) = \sum_{a \subseteq V} \xi_a(i_a), \quad (1)$$

where ξ_a are functions of cell i which only depend on the variables in a , i.e. on the so-called marginals i_a . These functions are called interactions between the variables in a . If $|a| = 1$, ξ_a is called main effect, if $|a| = 2$ first order interaction and an interaction of order $k - 1$ if $|a| = k$. For identifiability purposes we impose constraints on the functions, namely that k^{th} -order interaction functions are orthogonal to interaction functions of lower order.

A log-linear interaction model usually sets some of these functions equal to zero. Often, it is convenient to work with hierarchical models. These are interaction models where a vanishing interaction forces all interactions of higher order to be zero as well:

$$\xi_a = 0 \implies \xi_b = 0 \quad \text{for all } b \supseteq a$$

Hierarchical models can be specified via the so-called generators or generating class \mathcal{G} which is a set of subsets of V consisting of the maximal interactions which are present. Precisely, the generating class \mathcal{G} has the following property:

$$\xi_a = 0 \iff \text{there is no } q \in \mathcal{G} \text{ with } a \subseteq q. \quad (2)$$

In our example above with two binary factors, we may consider a model consisting of all main effects, an interaction between 1 and 2 and an interaction between 1 and 3: this corresponds to $\mathcal{G} = \{\{1, 2\}, \{1, 3\}\}$.

If we go back to formula (1) and rewrite it in matrix formulation, we get:

$$\log(\mathbf{p}) = \mathbf{X}\boldsymbol{\beta}, \quad (3)$$

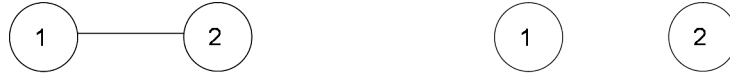
where $\boldsymbol{\beta}$ is a vector of unknown regression coefficients and $\mathbf{X} \in \mathbb{R}^{m \times m}$ the design matrix. Each row of \mathbf{X} corresponds to a certain cell and the columns of \mathbf{X} correspond to the functions $\xi_a(i_a)$. The number of columns needed to represent the function ξ_a depends on the number of different states i_a can take on. For example consider a categorical variable a that can take on 3 levels. Then, ξ_a is called a main effect (as $|a| = 1$) and X_a (the columns of \mathbf{X} corresponding to a) is 2-dimensional. Originally, it would be 3-dimensional but for identifiability purposes, the subspace spanned by X_a is chosen orthogonal to the already existing columns of lower order interaction (here orthogonal to the intercept) and we further choose it orthogonal within the subspace. By choosing the identifiability constraints this way, the parameterization of the matrix used in (3) is equivalent to choosing a poly contrast in terms of ANOVA. If we go back to our example with two binary factors where $m = 4$, (3) becomes:

$$\log \mathbf{p} \begin{pmatrix} (0, 0) \\ (0, 1) \\ (1, 0) \\ (1, 1) \end{pmatrix} = \mathbf{X}\boldsymbol{\beta}, \quad (4)$$

$$\text{with } \mathbf{X} = \begin{pmatrix} 1 & 1 & 1 & 1 \\ 1 & 1 & -1 & -1 \\ 1 & -1 & 1 & 1 \\ 1 & -1 & -1 & -1 \end{pmatrix}, \text{ and } \boldsymbol{\beta} = (\beta_0, \beta_1, \beta_2, \beta_{12}),$$

where the first column is the intercept and belongs to $a = \emptyset$, the second column belongs to $a = 1$ and has entry 1 whenever variable $a = 1$ takes on the first level and -1 else and similarly for the third column. The

Fig. 1 Graphical Models corresponding to the example given by formula (4). Left: full (saturated) model. Right: $\beta_{12} = 0$.



fourth column belongs to the interaction between variable 1 and 2. A description of \mathbf{X} for the general case can be found in Dahinden *et al.* (2007). In the following we will denote the components of β belonging to X_a with β_a .

In the next section, we will make the link between the generating class and graphical models.

2.2 Graphical Models

We first introduce some terminology. A graph is defined as a pair $G = (V, E)$, where V is the set of vertices or nodes and $E \subseteq V \times V$ is the set of edges linking the vertices. Each node represents a (categorical) random variable. Here we only consider undirected graphs which means that $(u, v) \in E$ is equivalent to $(v, u) \in E$. A path from u to v is a sequence of distinct nodes $v_0 = u, \dots, v_n = v$ such that $(v_i, v_{i+1}) \in E$ for all $i \in \{0, 1, \dots, n-1\}$. Given three sets of variables $A, S, B \subseteq V$, we say that S separates A from B in V if all paths from vertices in A to vertices in B have to pass through S . Consider a random vector $\mathbf{Z} = \{Z_v, v \in V\}$ with a certain distribution. We say that the distribution of \mathbf{Z} is globally Markov with respect to a graph G if for any 3 disjoint subsets $A, S, B \subseteq V$ the following property holds:

$$S \text{ separates } A \text{ from } B \implies Z_A \perp Z_B | Z_S, \quad (5)$$

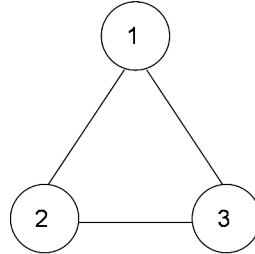
where the symbol “ \perp ” denotes (conditional) independence. This states that we can read off conditional independence relations directly from the graph if the distribution is globally Markov with respect to the graph and graphical models therefore provide a way to represent conditional (in)dependence relations between variables in terms of a graph structure. We say that a set of nodes of G forms a complete subgraph of G if every pair in that set is connected by an edge. A maximal complete subgraph is called a clique.

2.3 Graphical Models and Hierarchical Log-Linear Models

The undirected graphical model represented by a graph G corresponds to a hierarchical log-linear model where the cliques of the graph are the generators of the model. If we go back to our example in the previous section and assume that $\beta_{12} \neq 0$ in formula (4), then the hierarchical log-linear model (4) can be represented by the graphical model on the left side in Figure 1; and if $\beta_{12} = 0$, then the corresponding graphical model is the one on the right side in Figure 1.

On the other hand, assume that the generators of a log-linear model are given by a set \mathcal{G} . By connecting all the vertices appearing in the same generator, the so-called interaction graph builds up. By the definition of the interaction graph and by looking at formula (1), it becomes clear that the distribution induced by the log-linear model is Markov with respect to the interaction graph and we can read off conditional independences directly from the graph. It is also clear that \mathcal{G} corresponds to a graphical model via its interaction graph if and only if \mathcal{G} is the set of cliques of this graph. In that case we say that \mathcal{G} is a graphical generating class. If there are cliques in the interaction graph which are not in \mathcal{G} , the hierarchical log-linear interaction model is not graphical and its interaction structure cannot be adequately represented by the graph alone. However, the graph may still completely represent all conditional independencies of the underlying distribution. The simplest example of a hierarchical log-linear model which is not graphical is $V = \{1, 2, 3\}$ and $\mathcal{G} = \{\{1, 2\}, \{2, 3\}, \{3, 1\}\}$. Its interaction graph is shown in Figure 2 which has as its clique the complete graph $\{1, 2, 3\}$ and obviously, it is not equal to the set of generators \mathcal{G} . Any joint

Fig. 2 Example of an interaction graph corresponding to a hierarchical log-linear model which is not graphical.



probability distribution of discrete random variables can be expanded in terms of a log-linear interaction model. For some distributions it is possible to represent all (conditional) independencies in an undirected graphical model and these distributions are called faithful to their interaction graph G or we say that the graph is a perfect map of the distribution. In other words, the graph captures all and only the conditional independence relations of the distribution.

2.4 Collapsibility

Classifying objects into cells according to many categorical variables leaves us with high dimensional contingency tables. Analyzing such large contingency tables directly turns out to be difficult for two reasons. First, some of the cells are likely to be empty because of the exponentially growing amount of cells with growing number of variables, and this may lead to non-existence of the MLE estimator. Secondly, not only the number of cells is growing but also the number of parameters to estimate. Therefore it is often tempting to reduce the dimension of the table by collapsing over some variables if we want to determine the association between the remaining variables. Collapsing over a variable simply means summing over that variable and thereby to reduce (collapse) the table to the remaining dimensions. However in doing so, wrong associations between the variables may be introduced and original associations can vanish. Therefore, one has to be careful when collapsing is permitted and when it is not.

First, we define collapsibility in a precise sense.

Definition (Collapsibility): We say that a variable is collapsible with respect to a specific interaction ξ_a , when the interaction in the original contingency table is identical to the interaction in the collapsed contingency table.

The general result regarding collapsibility which goes back to a theorem stated in Bishop *et al.* (1975) can be summarized as follows:

By collapsing a table over a variable which interacts with s other variables, then s - and higher order interactions between the remaining variables are not changed in the collapsed table. (6)

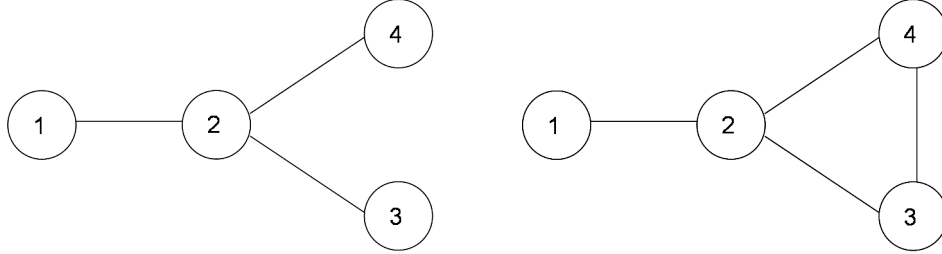
Conversely, lower-order interactions between the remaining variables are affected by collapsing.

For example, if we collapse over a variable which only interacts with one other variable no interaction changes by collapsing over that variable, but main effects may be changed. If we collapse over a variable which is independent of all other variables, then neither any main effects nor any interactions change.

2.5 Decomposability

As mentioned in Section 1, we will use a divide-and-conquer algorithm to perform model selection in log-linear interaction models. As we have seen, a graphical log-linear model has a corresponding graph which represents all conditional independencies. The graph may be decomposed into several subgraphs, where

Fig. 3 Left: Separating node 2 has corresponding index 2. Right: Separating node 2 has index 1.



each of the subgraphs is analyzed individually and the results can then be combined. The definition of such a decomposition is as follows:

Definition (Decomposition): A triple of disjoint subsets (A, S, B) of the vertex set V forms a decomposition if

1. $V = A \cup S \cup B$.
 2. S separates A from B .
 3. S is complete.
- (7)

Decomposability is defined recursively: A graph is decomposable if it is complete or if there exists a decomposition (A, S, B) where the subgraphs of G restricted to the vertex sets $A \cup S$ and $S \cup B$ are decomposable.

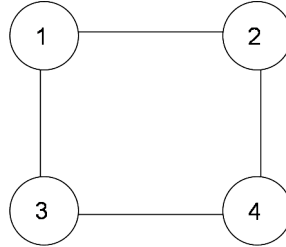
Denote by \mathcal{C} the set of all cliques of a decomposable graph and by \mathcal{S} the set of all separators. A decomposition consists of all cliques and separators \mathcal{C}, \mathcal{S} . As is proved for example in Lauritzen (1996), for a decomposable graph with decomposition into cliques \mathcal{C} and separators \mathcal{S} , the probability of a cell i is given by the following formula:

$$p(i) = \frac{\prod_{C \in \mathcal{C}} p(i_C)}{\prod_{S \in \mathcal{S}} p(i_S)^{\nu(S)}}, \quad (8)$$

where $\nu(S)$ is the so-called index of the separator. The formal definition of the index is a bit cumbersome and is given in the Appendix. However, intuitively it can be thought of as the number of times the set S acts as a separator. For example: on the left side of Figure 3, node 2 separates $\{1\}$ and $\{4\}$ (the cliques consisting of single nodes $\{1\}$ and $\{4\}$) and also separates $\{1\}$ and $\{3\}$. Therefore the index of the separating node 2 is 2, as the node 2 acts twice as separator. If we look at the right side of Figure 3, we see that the node 2 only separates $\{1\}$ from the clique $\{3, 4\}$ as the single nodes 3 and 4 are no longer cliques since there is an edge between them and therefore, the node 2 only acts once as separator and thus the corresponding index is 1.

2.5.1 Remark

It might not be possible to decompose the graph into decomposable (smaller) components. By definition, this is the case for non-decomposable graphs. The simplest example of a non-decomposable graph is given in Figure 4. But the analogue in the case of non-decomposable graphs is a decomposition into prime (irreducible) subgraphs. Prime subgraphs are graphs which do not admit a proper decomposition (7). A maximal prime subgraph is a prime subgraph with vertex set U where the subgraph with vertex set W is

Fig. 4 Example of a non-decomposable graph.

decomposable for all W with $U \subset W \subseteq V$. There exists a maximal prime subgraph decomposition (MPD) and it is unique. A prove as well as an algorithm to get the MPD is given in Olesen and Madsen (2002). The main idea behind the algorithm is to add a minimal number of edges to the graph, such that becomes decomposable (this step is called minimal triangulation), perform the decomposition and then aggregate the cliques again whose separators are incomplete. The remaining components are the prime components. An analogue of formula (8) with an MPD can then be derived.

3 Divide-and-Conquer Algorithm

The main problem of fitting a log-linear model, doing model selection in a log-linear model or fitting a graphical model to data is that it quickly becomes computationally infeasible with growing number of variables and growing number of levels per variable.

If we knew that the underlying graph is sparse, we could use a decomposition and collapse the contingency table on sub-tables given by the cliques \mathcal{C} and the separators \mathcal{S} given by the decomposition. Then we could perform model selection in the collapsed tables and combine the estimates according to formula (8). The problem is that we don't know the graph and therefore we don't know \mathcal{C} and \mathcal{S} for the decomposition. In the next section we propose a method how to come up with an initial graph estimate.

3.1 Selection of Marginal Models to Collapse on

A log-linear models measures the association among the variables. The association between two variables can be measured by doing regression from one variable upon the others. It is thus reasonable to apply a regression method to find groups of variables which are highly associated within a group but only weakly between groups. These groups of variables are the ones which we will collapse on. Inspired by Kim (2005), we use a nonparametric regression approach for finding these groups. But instead of using a single regression tree, we use a Random Forests approach Breiman (2001). The reason to use a regression- or classification-tree or a Random Forests approach consisting of such trees is that trees can naturally incorporate interactions between variables without running severely into the curse of dimensionality. For a detailed description of Random Forests see Breiman (2001).

3.1.1 Recursive Thinning of the Graph

Random Forests incorporates a way of measuring the importance of individual variables in explaining the response variable in a regression. For example, the importance measure can be the number of times a variable has been chosen as split variable (selection frequency) or the decrease in the so-called Gini index or the permutation accuracy which measures the prediction accuracy before and after permuting a variable. By doing regression from each variable on all others, a so-called importance matrix builds up. Assume we have a discrete random variable \mathbf{Z} consisting of Z_1, \dots, Z_d . The algorithm to build up the importance matrix is:

Set $impat = d \times d$ matrix consisting of 0

For i **in** $1:d$

Do regression $Z_i \sim \mathbf{Z} \setminus Z_i$

Set $impat[i, -i] \leftarrow$ importance of regression

Return $impat$

A high entry in the importance matrix indicates a strong association between the corresponding row and column variable. However, one has to be careful in choosing the importance criteria as far as comparability of the importance between various predictor variables as well as between different regressions is concerned. It has been shown that the popular importance criteria in Random Forests such as the Gini index, selection frequency or the permutation accuracy importance measure are all strongly biased towards variables with more categories (see Strobl *et al.* (2007)). We therefore propose to use the cforest method proposed by Strobl *et al.* (2007) which provides a variable importance measure that can be reliably used for variable selection even in situations where the predictor variables vary in their scale of measurement or their number of categories. However, the importance measures are only consistent within rows but not between rows as the variable importance not only depends on the predictor variables in a regression but also on the response variable and therefore, they cannot be directly compared between rows. For that reason we only consider the ranks of the importance matrix entries within rows, meaning that the smallest entry in a row has rank 1, the next higher has rank 2 and so on. The idea is that if two variables i and j are strongly (conditionally) dependent, then j has high rank in explaining i and the other way round, meaning that the $impat_{i,j}$ and $impat_{j,i}$ entries are both large.

We then recursively eliminate the edges with lowest corresponding importance matrix entry. Thereby we only eliminate the edge if both entries (i, j) and (j, i) pointing to the variables i and j are below a certain threshold, as the importance matrix is not symmetric. When doing so, we start from the full graph and successively eliminate edges.

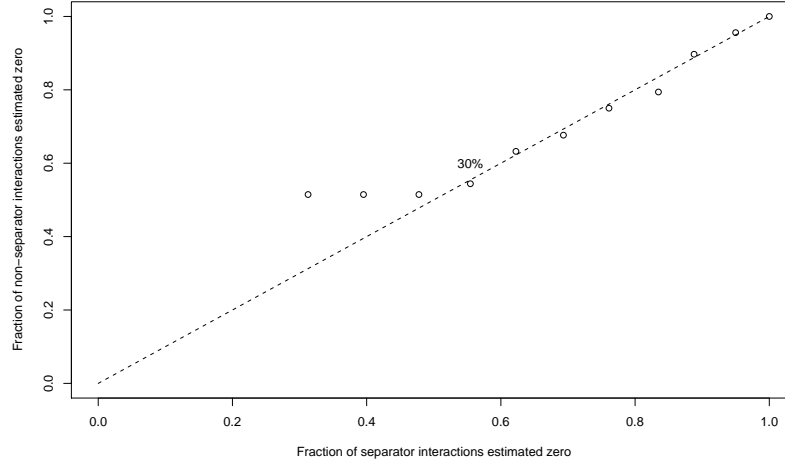
3.1.2 Decomposition

Whenever an edge is deleted in the process of the recursive thinning procedure from Section 3.1.1, we decompose the graph according to formula (7). For non-decomposable graphs we decompose the minimal triangulation of the graph, which means we add edges to the graph until it becomes decomposable (minimal triangulation) and don't perform the aggregation step described in Section 2.5.1. Formula (8) also holds for such a triangulated graph. The reason for doing so is that at this point we are not interested in an optimal decomposition, but we only want to decompose the graph into smaller subgraphs for which we have the computational capacity to fit a log-linear model. Therefore it is not crucial that we have the sparsest possible subgraphs to collapse on. It is only important that the size of the graph to collapse on is appropriate for our problem and then, any reasonable log-linear model selection procedure can be applied for these subgraphs. If a clique in the (triangulated) thinned graph is small enough, e.g. for binary variables this might be the case for around 10 variables, we split off part of this clique and only proceed with the remaining sub-graph. In detail, if $A \cup S$ corresponds to a clique in the (triangulated) thinned graph, where S separates A from $V \setminus \{A \cup S\}$ and say the number of nodes in $A \cup S$ is less or equal to 10, then we split off the nodes in A . We proceed that way (recursively deleting edges, decomposing the thinned graph and trying to split off cliques) until the graph decomposition of the remaining variables consists of cliques which are small enough to be able to perform log-linear model selection.

3.2 Combination of results

Assume we have collapsed the table on the cliques \mathcal{C} and separators \mathcal{S} of the graph induced by the recursive thinning and decomposition procedure. Furthermore, assume that we have fitted a model for each of these

Fig. 5 Illustration of how many separator edges to take up into the model. x-axis: the fraction of separator interactions ξ with $\hat{\beta}_\xi = 0$ among all separator interactions. y-axis: the fraction of non-separator interactions with estimated interaction coefficient equal zero. The points correspond to different levels of thresholding. We see that if we threshold 30% of the non-zero $\hat{\beta}$ coefficients, we have almost exclusively thresholded separator interactions, as we would expect.



sub-tables (the collapsed tables on \mathcal{C} and \mathcal{S}). We then get the log-linear model corresponding to the full graph by using formula (8):

$$\begin{aligned}
 \log p(i) &= \sum_{C \in \mathcal{C}} \log p(i_C) - \sum_{S \in \mathcal{S}} \nu(S) \log p(i_S) \\
 &= \sum_{C \in \mathcal{C}} X_C \beta_C - \sum_{S \in \mathcal{S}} \nu(S) X_S \beta_S,
 \end{aligned} \tag{9}$$

where X_C and X_S are the design matrices resulting from restricting the total design matrix to nodes in C and S respectively. The same notation applies to β_C and β_S . Formula (9) describes how to aggregate the results of the collapsed tables. In addition, one can derive from (9) that if we have 3 disjoint subsets A, S, B where S separates A from B , then we can safely collapse over B without changing an interaction between variables in A or between variables consisting of a mix of A and S . The only interactions which might change are the ones between variables which are exclusively in S (in the following denoted by separator interactions). This is in accordance with the result stated in Section (6). However, if we do model selection for all sets in \mathcal{C} and \mathcal{S} , we typically get a model which is too big. The reason for this is that, as mentioned above, if we have a decomposition (A, S, B) of V , then collapsing on the set A might introduce interactions between variables which are exclusively in S (separator interactions might be changed). But as formula (9) holds, the introduced interactions have a very small β coefficient. We therefore expect that if we threshold the interaction vector, most of the introduced zeros belong to so-called separator interactions $\xi: \exists S \in \mathcal{S}$ with $\xi \in S$, i.e. interactions exclusively contained in a separator. Consequently, we set the threshold that the introduced zeros belong to equal parts to separator- and non-separator interactions. See Figure 5 for a graphical illustration of the procedure. In Section 5.1.2 we will argue empirically that such a thresholding rule works well.

4 Graphical Model Selection Procedures

We distinguish between divide-and-conquer (decomposition) and global approaches: thereby, divide-and-conquer (decomposition) methods refer to approaches where the graph is decomposed as described in Section 3.1.2 and any graphical model selection procedure described in Section 4.1 below is used. In contrast, a global method does not involve such a decomposition and the global approaches used here are described in Section 4.2.

4.1 Model Selection Procedures used in Combination with the Decomposition Approach

4.1.1 ℓ_1 -Regularized Model Selection

Inspired by the Lasso, originally formulated by Tibshirani (1996) for estimation and variable selection in linear regression, a model selection approach for log-linear models has been developed in Dahinden *et al.* (2007).

The coefficient vector β is estimated with the group- ℓ_1 -penalty (Yuan and Lin, 2006):

$$\hat{\beta}^\lambda = \arg \min_{\beta} \left[-\frac{1}{n} l(\beta) + \lambda \sum_{\substack{a \subseteq C \\ a \neq \emptyset}} \|\beta_a\|_{\ell_2} \right], \quad (10)$$

where $l(\beta) = \sum_{i=1}^m n_i (\mathbf{X}\beta)_i = \log \mathbb{P}_{\beta}[\mathbf{n}] + c$. Therefore $l(\beta)$ is up to an additive constant c , which does not depend on β the log-likelihood function. This minimization has to be calculated under the additional constraint that the cell probabilities add to 1:

$$\sum_{i=1}^m \exp \{(\mathbf{X}\beta)_i\} = 1.$$

The group- ℓ_1 -penalty

$$\sum_{\substack{a \subseteq C \\ a \neq \emptyset}} \|\beta_a\|_{\ell_2}, \text{ where } \|\beta_a\|_{\ell_2}^2 = \sum_j (\beta_a)_j^2,$$

has the property that the solution of (10) is independent of the choice of the orthogonal subspace of X_a and furthermore, the penalty encourages sparsity at the interaction level, meaning that the vector $\hat{\beta}_a$ corresponding to the interaction ξ_a has all components either non-zero or zero. In addition, by using group- ℓ_1 model selection we avoid the sampling zero problem, which is problematic regarding the existence of the MLE (see e.g. Christensen (1991)).

The tuning parameter λ can be assessed by cross-validation: we divide the individual counts into a number of equal parts and in turn leave out one part and use the rest to form a training contingency table with cell counts \mathbf{n}_{train} .

4.1.2 Stepwise Forward

The stepwise forward procedure aims to minimize the AIC-type criterion $sk - 2 \log(l)$, where l is the maximized value of the likelihood function for the corresponding model with k degrees of freedom; $s = 2$ corresponds to the genuine AIC. Here we also vary the parameter s ; a large parameter leads to sparser models and if $s = 0$ generally the saturated model is chosen.

4.2 Global Model Selection Procedures

4.2.1 Wainwright et al. Method

In Wainwright *et al.* (2007) the problem of estimating the graph structure of binary valued Markov networks is considered. They propose to estimate the neighborhood of any given node by performing ℓ_1 -penalized logistic regressions on the remaining variables. Assume we have d binary random variables and observations thereof $z = (z_1, \dots, z_d) \in \{0, 1\}^d$. Furthermore, we assume that the data are generated under the so-called Ising model:

$$\log p(\mathbf{z}) = \sum_{s,t=1}^d \theta_{st} z_s z_t + \Psi(\Theta), \quad (11)$$

where Θ is a symmetric $d \times d$ matrix and $\Psi(\Theta)$ is a normalizing constant which ensures that the probabilities add up to one. This constant is also known as the log-partition function. If we go back to the log-linear interaction model described in Section 2.1 with binary variables, i.e. the cell $i \in \{0, 1\}^d$, then by comparing formula (1) to (11) we see that the Ising model is a log-linear model whose highest interactions are of order one and the parameterization is, in terms of ANOVA, with Helmert instead of poly contrasts. Therefore, the interaction graph builds up by connecting the nodes s and t for which $\theta_{st} \neq 0$. If we go back to the example in Section 2.1 where the two random variables are binary and rewrite formula (11) in matrix formulation we get:

$$\log \mathbf{p} \begin{pmatrix} (0, 0) \\ (0, 1) \\ (1, 0) \\ (1, 1) \end{pmatrix} = \mathbf{X} \begin{pmatrix} \Psi(\theta) \\ \theta_{11} \\ \theta_{22} \\ 2\theta_{12} \end{pmatrix}, \text{ with } \mathbf{X} = \begin{pmatrix} 1 & 0 & 0 & 0 \\ 1 & 0 & 1 & 0 \\ 1 & 1 & 0 & 0 \\ 1 & 1 & 1 & 1 \end{pmatrix}. \quad (12)$$

By comparing (12) to (4) we see that the normalizing constant $\Psi(\theta)$ corresponds to the intercept β_0 , θ_{11} to the main effect β_1 , θ_{22} to the main effect β_2 and $2\theta_{12}$ corresponds to the first order interaction β_{12} .

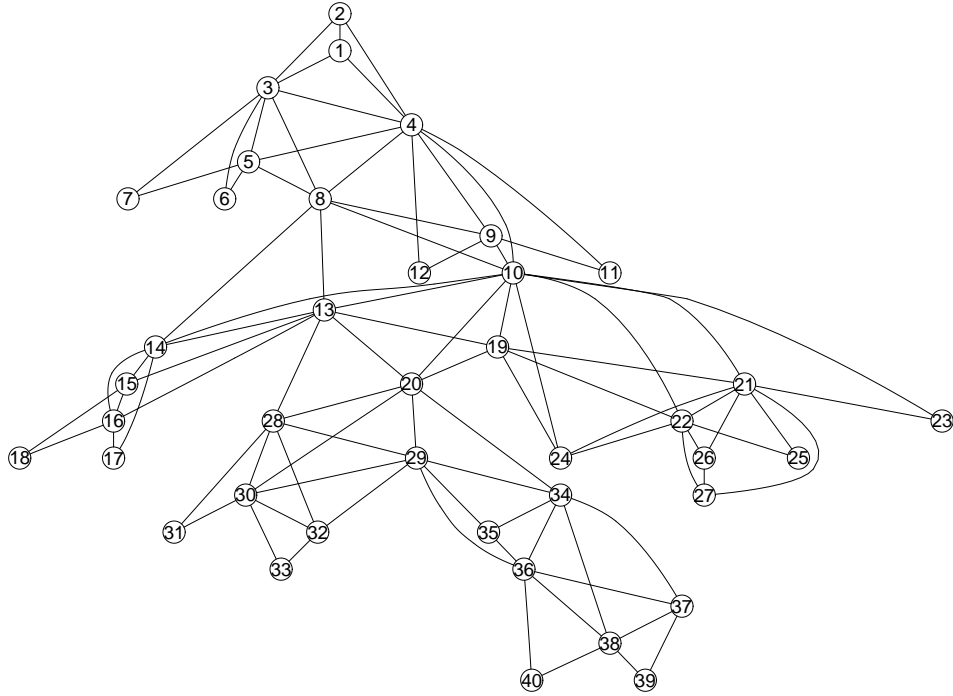
It holds that:

$$\log \left(\frac{p(z_s = 1 | z_{\setminus s})}{p(z_s = 0 | z_{\setminus s})} \right) = \theta_{ss} + \sum_{t=1, t \neq s}^d 2\theta_{st} z_t, \quad (13)$$

and therefore, we can infer the matrix θ by doing d logistic regressions from each variable on the remaining variables: θ_{ss} is then the intercept in the logistic regression from z_s on the remaining variables $z_{\setminus s}$ and $2\theta_{st}$ equals the regression coefficient corresponding to z_t . Furthermore, Wainwright *et al.* (2007) apply ℓ_1 -penalized logistic regression to estimate the θ -matrix. However, the resulting θ is not necessarily symmetric and it has to be symmetrized for example by taking the maximum of θ_{st} and θ_{ts} . Furthermore, Wainwright *et al.* (2007) prove that under certain sparsity assumptions their method correctly identifies the underlying graph structure. We emphasize that the Wainwright *et al.* (2007) approach works for binary variables only, while the decomposition approaches in Section 4.1 work for general multi-category variables.

4.2.2 Random Forests (global)

Random Forests (Breiman, 2001) is a regression method which internally calculates variable importances and these variable importances can be used to build an importance matrix. The exact procedure how this matrix is built, is explained in Section 3.1.1. We recursively eliminate edges with least importance like in the recursive thinning process described in Section 3.1.1 to get sparser graphs. This yields a graph but no estimation of the log-linear interaction model is provided.

Fig. 6 Graph from which we simulate.

5 Simulation Study

We simulate from a log-linear interaction model corresponding to a graph with 40 nodes and 91 edges. Each node corresponds to a binary variable (and thus, we can compare with the method in Wainwright *et al.* (2007)). The graph is displayed in Figure 6. This is the same simulation setting as was used in Kim (2005). We generate 10 datasets each consisting of 10000 observations according to the graph in Figure 6. We restrict the log-linear model selection procedure to first order interaction models even though the true underlying graph includes interactions of higher order. Projecting a general log-linear model involving higher order interactions to the best (w.r.t. the Kullback-Leibler divergence) first-order interaction model, yields a log-linear model with non-zero first-order interaction coefficients. This implies that we can identify the true graph even though we restrict ourselves to first order interactions.

5.1 Results

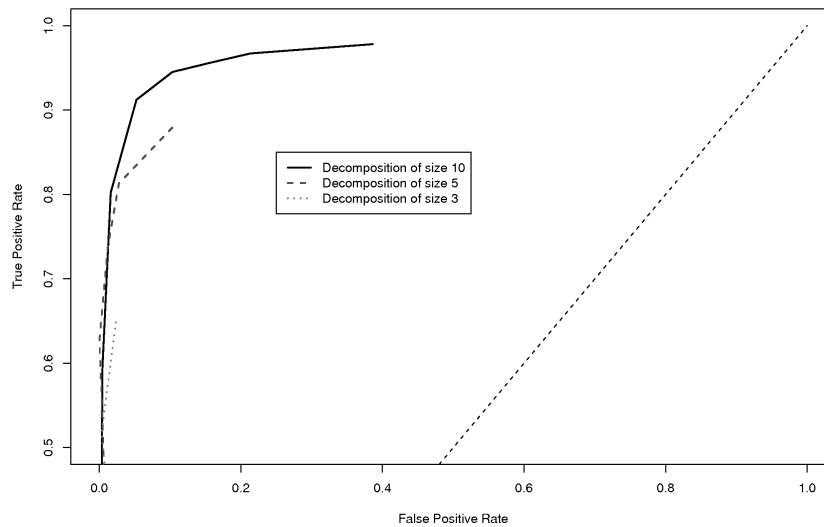
In Section 5.1.1 we compare the approaches with respect to performance in estimating the correct model structure and in Section 5.1.2 with respect to accuracy for estimating the parameter vector.

5.1.1 Model Selection Performance for the Graph

First, we assess in Figure 7 the optimal decomposition size. We decompose (with Random Forests) the graph into several subgraphs using different decomposition sizes (maximal size of cliques equal to 3,5 and

10), then use the ℓ_1 -penalization approach described in Section 4.1.1 to estimate the log-linear model for each subgraph and combine these results as described in Section 3.2. An ROC curve is drawn, where the endpoints of the curves correspond to the selected model with λ in (10) chosen by cross-validation. The curves correspond to models which arise by successively eliminating edges with smallest interaction vector coefficient. We see here that larger decomposition sizes lead to slightly more favorable ROC curves. The picture remains qualitatively the same if we use stepwise forward instead of ℓ_1 -penalization.

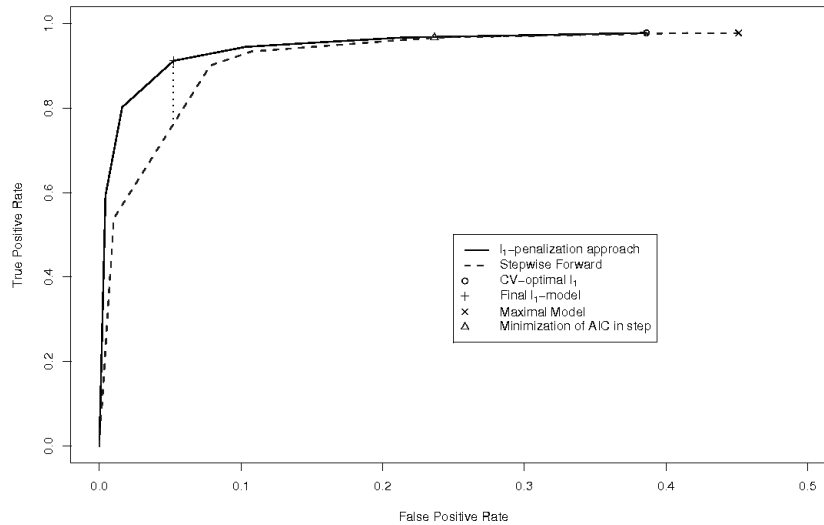
Fig. 7 Comparison of decomposition sizes. Decomposition into cliques of maximal size 3, 5 and 10 with Random Forests and subsequent model selection with ℓ_1 -penalization. The curves corresponds to models which arise by thresholding the final $\hat{\beta}$ -coefficient.



In Figure 8, ℓ_1 -penalization and the stepwise forward method are compared after the decomposition with Random Forests using maximal clique size equal to 10. For the stepwise forward method the line builds up by varying s (compare Section 4.1.2), while the ℓ_1 -penalization approach starts from the CV-solution (endpoint of the curve) and uses hard-thresholding of $\hat{\beta}$ for obtaining the values on the ROC curve. We see that the stepwise forward and the ℓ_1 -penalization approach lead to models which have approximately the same number of false positive and false negative edges, but the ℓ_1 -approach is slightly favorable. However, if we threshold the $\hat{\beta}$ coefficients of the AIC ($s=2$) solution, the line of the stepwise forward approach is very close to the ℓ_1 solution (not shown here). Note that in Figure 8 the black cross indicates the final selected ℓ_1 -solution if the thresholding procedure described in Section 3.2 is applied.

In Figure 9, the global approaches (Wainwright *et al.* (2007) and global Random Forests regression from Section 4.2.2) are compared with the ℓ_1 -penalization decomposition approach. In order to keep a simple overview, the line for the stepwise procedure is no longer drawn. We see that our decomposition approach slightly outperforms the global approaches (but the global Random Forests does not yield an estimate for the parameter vector and the method from Wainwright *et al.* (2007) does so only for binary variables). If we assess the optimal λ parameter for the method from Wainwright *et al.* (2007) in each regression with cross-validation, we get a model which is close to the saturated model as we can see by

Fig. 8 Comparison of decomposition approaches. The graph is decomposed into cliques of maximal size 10 and then ℓ_1 -penalization and stepwise forward model selection is applied to the subgraphs before they are combined using formula (9). The dotted line corresponds to the difference in the true positive rate for the two procedures when the two procedures are compared at the false positive rate of the final ℓ_1 -penalization model.



the red cross indicated in Figure 9. Even though Figures 8 and 9 only represent one simulated dataset, the picture doesn't change for other simulations. The lines for the stepwise and the ℓ_1 approach are always very close, with the ℓ_1 -penalization method slightly better and both methods clearly superior to the global approaches. The reason why Figures 8 and 9 only display results from one dataset is that the single final models cannot be averaged over different datasets as they have different positions on the curves for different datasets (different numbers of true and false positives), and if we average over all these values, the result is not very meaningful anymore. However, we can average the differences of true positive rates for e.g. the final ℓ_1 -penalized model and the stepwise model with the same number of false positives as the ℓ_1 -solution (dotted line in Figure 8). The results of such comparisons are summarized in Table 1. We see that the final ℓ_1 -penalization decomposition solution yields a significantly higher true positive rate than the corresponding stepwise solution. On the other hand, the comparison between the AIC solution and the corresponding (in terms of false positives) ℓ_1 -solution shows that there is no significant difference.

The stepwise decomposition method, the ℓ_1 -decomposition approach as well as the global method in Wainwright *et al.* (2007) yield estimates of the interaction vector β (for the ℓ_1 - and the stepwise forward approach) or θ (for the Wainwright approach). In the next section we will compare these methods with respect to the performance for estimating the parameter vector β .

5.1.2 Comparison of Parameter Estimation

All approaches considered here yield the interaction vector β only up to a constant (except for global Random Forests which does not yield an estimate of β). For the method in Wainwright *et al.* (2007),

Fig. 9 Comparison of global approaches (Wainwright *et al.* (2007) and global Random Forests from Section 4.2.2) with ℓ_1 -penalization decomposition and stepwise forward decomposition approaches. For the ℓ_1 -penalization decomposition approach, the line builds up by thresholding the $\hat{\beta}$ -coefficient where λ is chosen by CV. For Random Forests, the edges with least importance are successively eliminated and for the Wainwright *et al.* method, the tuning parameter λ is varied.

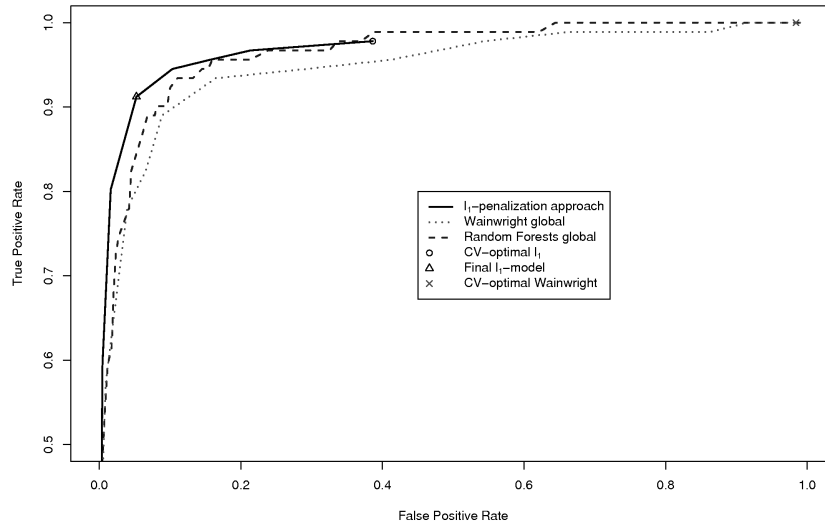


Table 1 Comparisons of true positive rates between the final ℓ_1 -penalization decomposition solution (denoted by “ ℓ_1 final”) and the corresponding (in terms of false positives) solutions of other methods (denoted by “Stepwise”, “Wainwright” and “Random Forests”). In addition the AIC solution from the stepwise decomposition approach is compared to the corresponding ℓ_1 -penalization decomposition solution (“Stepwise AIC - ℓ_1 ”).

	Mean difference	p-value (t-test)
ℓ_1 final - Stepwise	0.052	0.036
ℓ_1 final - Wainwright	0.060	0.011
ℓ_1 final - Random Forests	0.013	0.256
Stepwise AIC - ℓ_1	0.002	0.512

the constant $\Psi(\Theta)$ given in formula (11) is not computed at all. For the stepwise as well as for the ℓ_1 -penalization method we ensure that the probabilities add up to one in each submodel, but when combining the models according to formula (9) this property only holds approximately. The reason is that we do not consistently estimate the marginal distributions, i.e. for a decomposition $V = (A, S, B)$ we require that $\sum_{x_A} \hat{p}_{A,S}(x_A, x_S) = \sum_{x_B} \hat{p}_{B,S}(x_B, x_S)$, but this is only fulfilled approximately. Thus, we need to normalize. For sparse graphs, we can use the junction tree algorithm to calculate the constant. We know that the probability distribution can be represented by a product of clique marginal distributions divided by the product of separator distributions. The junction tree algorithm constructs a junction tree from the

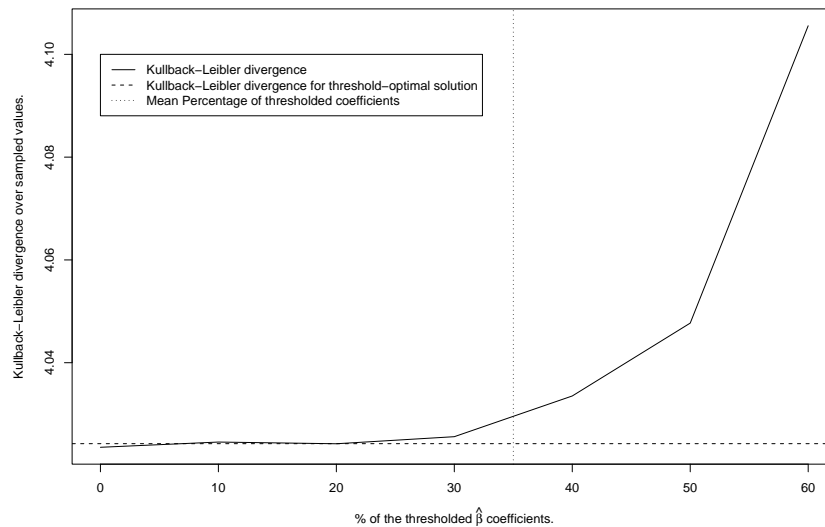
graph, we can then assign potentials for each cluster of the tree and by message propagation on the tree, the potentials are transformed to consistent marginal probabilities such that we can calculate the normalizing constant. For a detailed description see Lauritzen (1996).

We compare the estimated probabilities using an expression which is up to a constant the Kullback-Leibler divergence between the estimated and the true probability (non-normalized Kullback-Leibler divergence):

$$-\log \left(\prod_i \hat{p}_i^{p_i} \right) = -\sum_i p_i \log \hat{p}_i, \quad (14)$$

where $\hat{\mathbf{p}}$ is the estimated probability vector and \mathbf{p} denotes the true probability vector. As this sum requires the calculation of $2^{40} \approx 10^{12}$ components of $\hat{\mathbf{p}}$ and \mathbf{p} and the summation of the two huge vectors, this is computationally not feasible. To avoid this problem, we calculate an empirical version by simulating one million observations from the graph in Figure 6 and summing over these values only. The results are sum-

Fig. 10 Mean empirical (non-normalized) Kullback-Leibler distance between true and estimated probability in dependence of the percentage of thresholded coefficients. The vertical line indicates the average of percentages of thresholded coefficients using the thresholding rule from Section 3.2.



marized in Table 2. In this table we have included our three estimators: the two decomposition approaches denoted by “ ℓ_1 -penalization” and “stepwise forward” and the global “Wainwright et al.” approach. In addition we have included the “full decomposition model”, where no model selection is performed after decomposition and MLE on the decomposed model is used. Again, we see that the ℓ_1 -penalization approach and the stepwise forward approach perform similarly and the approach in Wainwright *et al.* (2007) is clearly inferior. The Wainwright solution listed in Table 2 is the solution for the minimal λ for which the normalization constant could be computed. This solution is also indicated in Figure 8. For the CV-optimal solution, which is indicated in Figure 8, the normalizing constant cannot be computed as the junction tree algorithm does hardly provide a simplification due to the fact that the CV-optimal solution almost

corresponds to the full model. However, the maximal computable solutions correspond to very large models, which on average involve 22.05% of all possible edges, compared to 17.01% for the ℓ_1 -solution and 11.66% for the true graph.

Table 3 provides further insight about significance of the differences in Table 2. All methods are compared against each other using a paired t-test for the empirical (non-normalized) Kullback-Leibler divergences. The p -values are listed in Table 3. One can see that there is no significant difference for the decomposition approaches (ℓ_1 -penalization, stepwise forward and the full decomposition model using MLE for the decomposed models), whereas they are all superior over the approach in Wainwright *et al.* (2007). This provides evidence that the decomposition of the model is more crucial than the effective choice of the log-linear model fitting procedure afterwards.

Furthermore, it is worthwhile stating that the thresholding of the coefficients (see Section 3.2) does hardly influence the likelihood as we can see in Figure 10. On average, 35% of the coefficients are thresholded as indicated by the dotted line. However, for these threshold-optimal solutions, calculated as described in Section 3.2 (see also Figure 5), the empirical (non-normalized) Kullback-Leibler divergence is approximately the same as for the non-thresholded model (see Figure 10).

Table 2 Mean empirical (non-normalized) Kullback-Leibler divergence between true and estimated probabilities. The p -values for all the pairwise comparisons are given in Table 3.

	Mean	SD
ℓ_1 final	4.0080	0.0204
Stepwise AIC	4.0242	0.0217
Full decomp. model	4.0223	0.0099
Wainwright et al.	4.3360	0.1094

Table 3 All possible pairwise comparisons between models: p -values of a paired t-test for the equality of (non-normalized) Kullback-Leibler divergence.

	Stepwise AIC	Full decomp. model	Wainwright
ℓ_1 final	0.1030	0.0677	$4.7 \cdot 10^{-6}$
Stepwise AIC	-	0.8080	$6.0 \cdot 10^{-6}$
Full decomp. model	-	-	$7.5 \cdot 10^{-6}$

6 Application to Tissue Microarray Data

6.1 Tissue Microarray Technology

The central motivation that led to this work was to fit a graphical model to discrete expression levels of biomarkers resulting from Tissue Microarray (TMA) experiments. Tissue Microarray technology allows rapid visualization of molecular targets in thousands of tissues at a time, either at DNA, RNA or protein level. Tissue Microarrays are composed of hundreds of tissue sections from different patients arrayed on a single glass slide. With the use of immunohistochemical staining, they provide a high-throughput method to analyze potential biomarkers on large patient samples. The assessment of the expression level of a biomarker is usually performed by the pathologist on a categorical scale: expressed/not expressed, or the level of expression.

Tissue Microarrays are powerful for validation and extension of findings obtained from genomic surveys such as cDNA microarrays. cDNA microarrays are useful to analyze a huge number of genes, e.g. a couple of thousands in one specimen at a time. In contrast, TMAs are applicable to the analysis of one target at a time, denoted as biomarker, but in up to 1000 tissues on each slide. The

applicable to the analysis of one target at a time, denoted as biomarker in the following, at a time, but in up to 1000 tissues on each slide. The analysis of the interaction pattern of these biomarkers and in particular the estimation of the graphical model associated with the underlying discrete random variables are of bio-medical importance. These graph-based patterns can deliver valuable insight into the underlying biology. A detailed description of the Tissue Microarray technology can be found in Kallioniemi *et al.* (2001).

6.2 Data

Our TMA dataset consists of Tissue Microarray measurements from renal cell carcinoma patients. We have information from 1116 patients, 831 thereof having a clear cell carcinoma tumor, which is the tumor of interest here. We have identified 18 biomarkers from which we have information for the majority of the patients. Among 831 ccRCC (clear cell renal cell carcinoma) observations, 527 observations are complete with all biomarker measurements available. For 87 observations one measurement was missing, 64 and 30 observations had 2 or 3 missing values, respectively. 123 observations contained more than 3 missing values and were ignored in the analysis. For the observations with 1, 2 or 3 missing values, multiple imputation was applied using the R package mice (Van Buuren and Oudshoorn, 2007). From 18 biomarkers, 9 are binary and 9 have 3 levels.

6.3 Graphical Model

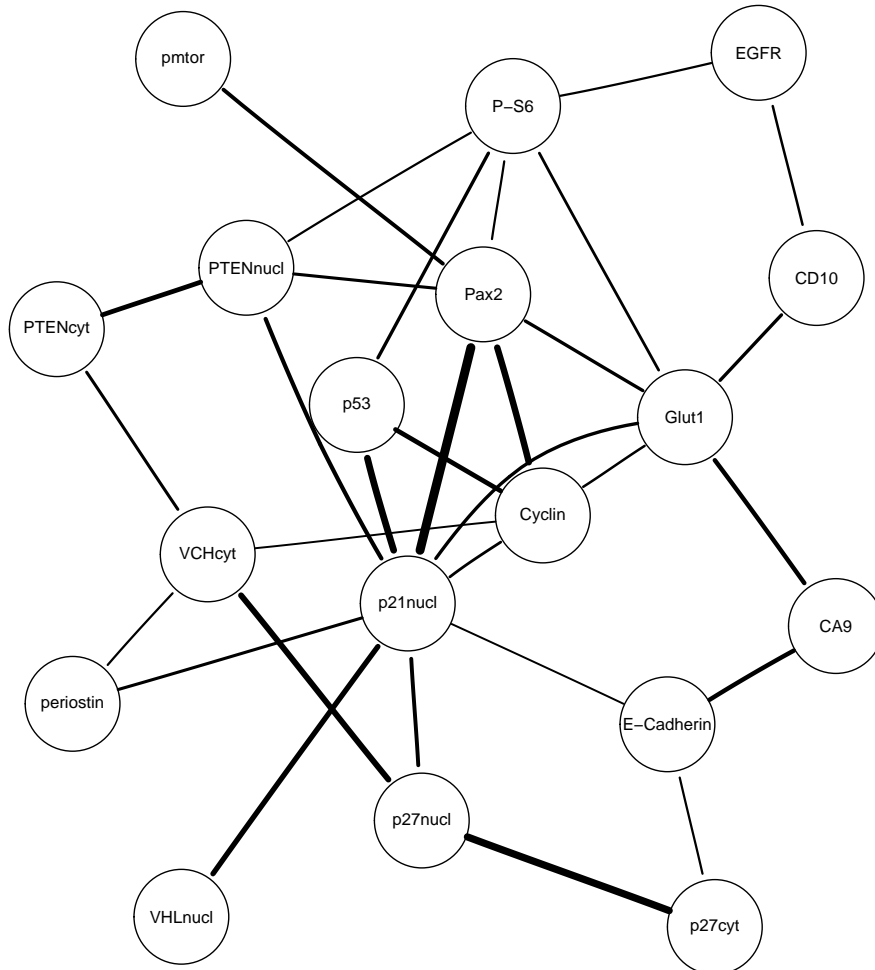
The graphical model corresponding to the TMA data is displayed in Figure 11. The thickness of the line corresponds to the ℓ_2 -norm of the respective interaction coefficients. Two biomarkers connected by a thick line, as is the case for nuclear p27 and cytoplasmic p27, indicates a strong interaction. The kinase inhibitor p27 exhibits its function in the cell nucleus and therefore recent studies have focused on nuclear p27 expression. Our graphical log-linear model however shows a tight association between nuclear and cytoplasmic expression of p27. Therefore it can be speculated that both nuclear and cytoplasmic presence is required to ensure proper function of p27. It has been shown that in renal tumors, the von Hippel-Lindau protein (VHL protein) is upregulating the expression of the tumor suppressor p27 (Osipov *et al.*, 2002). The graphical model here provides supporting evidence that VHL indeed regulates p27, and the corresponding β coefficient (not displayed here) implies that it is a positive regulation.

Furthermore it has been shown in vitro by Roe *et al.* (2006) that VHL increases p53 expression which is a tumor suppressor. In our model it seems as if p53 is conditionally independent of VHL. Indeed, it has long been known that p53 activates expression of p21 (e.g. Kim (1997)). This dependence is displayed very clearly in the graphical model. We can therefore view the p53-p21 pathway with its strong interaction as one unit and it is therefore very reasonable that nuclear VHL interacts with p53. As nuclear VHL is only expressed in 14% of the tumors, and it further makes sense from a biological point of view that the strong interaction between VHL and the p21-p53 pathway is in fact a causal relation, we can indeed speculate that the loss of VHL deactivates the tumor suppressor p53 which in turn favors tumor development.

CA9, Glut1 and Cyclin D1 are all hypoxia-inducible transcription factor (HIF) target genes (Wenger *et al.*, 2005). HIF has not been measured but we can clearly see that all these HIF targets are connected by a rather thick line implying that they might react to a common gene. In addition, CD10 strongly interacts with Glut1 a known HIF target which suggests that CD10 might also be regulated by HIF. The reduction of E-Cadherin expression has been found to be negatively correlated with HIF expression in Imai *et al.* (2003). This is supported by a strong negative interaction between E-Cadherin and CA9 which is positively correlated with HIF expression (not measured).

A lot of supporting evidence has been delivered for already existing theories. However, two strong interactions, one between PAX2 and nuclear p21 and the other between PAX2 and Cyclin D1 cannot be immediately explained. PAX2 is absent in normal renal tubular epithelial cells but expressed in many clear cell renal cell carcinoma tumours (see Mazal *et al.* (2005)). Its frequent expression together with the strong interaction with the p21-p53 pathway, Cyclin D1 and PTEN make PAX2 an interesting and possibly important molecular parameter whose exact function and role still remains to be elucidated.

Fig. 11 Estimated graphical model from Tissue Microarray data



7 Discussion

We have proposed a divide-and-conquer procedure to estimate log-linear models for large contingency tables and for fitting discrete graphical models. In a simulation study we have compared various algorithms and concluded that the divide-and-conquer procedures are very powerful. It seems that the decomposition of the problem is much more crucial than the choice of the algorithm to handle the smaller decomposed datasets; no matter whether ℓ_1 -penalized model selection, stepwise forward model selection or no model selection but only parameter estimation is applied after the decomposition, the resulting models are clearly superior to global (non-decomposition) approaches for model selection as well as for probability or parameter estimation.

Maybe most important is the computational feasibility of our procedure for large contingency tables with factors having more than two levels. The proposed method is scalable to orders of realistic complexity (e.g. dozens up to hundreds of factors) where most or all other existing algorithms become infeasible. In particular, our procedure is not only capable of handling binary data but can easily deal with factors with more levels. Furthermore, with the ℓ_1 -penalization procedure one doesn't risk the nonexistence of the parameter estimator in case of sampling zeroes in the contingency table as this might arise in MLE. In summary, we propose a procedure which is capable of handling a large amount of variables and there is hardly any limitation for the sample size n . The procedure not only fits a graphical model but also yields an estimation of the interaction vector β in a log-linear model and therefore of the cell probabilities. All this is achieved with good performance in comparison to other methods. As a drawback, if the true underlying graph has a clique which is larger than our decomposition size, then some of the edges in the graph are necessarily lost.

We apply the proposed approach to a problem in molecular biology and we find supporting evidence for dependencies between biomarkers which have already been found to exist in vitro or some even in renal tumors, the domain of our application. However, some strong interactions cannot be explained immediately and therefore, new biological hypotheses arise.

An R package called *decompgraph* where the decomposition and the graphical model selection procedure presented in this article is implemented will be available for download.

Acknowledgements We would like to thank Dr. Peter Schraml for comments, suggestions and discussions regarding biological interpretation.

References

- Bishop, Y., Fienberg, S. and Holland, P. (1975) *Discrete Multivariate Analysis*. MIT Press, Cambridge, Massachusetts and London, UK.
- Breiman, L. (2001) Random forests. *Machine Learning*, **45**, 5–32.
- Christensen, R. (1991) *Linear Models for Multivariate Time Series, and Spatial Data*. Springer-Verlag.
- Dahinden, C., Parmigiani, G., Emerick, M. and Bühlmann, P. (2007) Penalized likelihood for sparse contingency tables with an application to full-length cDNA libraries. *BMC Bioinformatics*, **8**, 476.
- Darroch, J., Lauritzen, S. and Speed, T. (1980) Markov fields and log-linear interaction models for contingency tables. *Ann. Statist.*, **8**, 522–539.
- Imai, T., Horiuchi, A., Wang, C., Oka, K., Ohira, S., Nikaido, T. and Konishi, I. (2003) Hypoxia Attenuates the Expression of E-Cadherin via Up-Regulation of SNAIL in Ovarian Carcinoma Cells. *The American Journal of Pathology*, **163**, 1437–1447.
- Jackson, L., Gray, A. and Fienberg, S. (2007) Sequential category aggregation and partitioning approach for multi-way contingency tables based on survey and census data. *submitted to Annals of Applied Statistics*.

- Kallioniemi, O., Wagner, U., Kononen, J. and Sauter, G. (2001) Tissue microarray technology for high-throughput molecular profiling of cancer. *Hum. Mol. Genet.*, **10**, 657–662.
- Kim, S. (2005) Log-linear modelling for contingency tables by using marginal model structures. Research Report 05, Division of Applied Mathematics, Korea Advanced Institute of Science and Technology.
- Kim, T. (1997) In vitro transcriptional activation of p21 promoter by p53. *Biochemical and Biophysical Research Communication*, **234**, 300–302.
- Lauritzen, S. (1996) *Graphical Models*. Oxford Statistical Science Series, 17. Oxford Clarendon Press.
- Mazal, P., Stichenwirth, M., Koller, A., Blach, S., Haitel, A. and Susani, M. (2005) Expression of aquaporins and pax-2 compared to cd10 and cytokeratin 7 in renal neoplasms: a tissue microarray study. *Modern Pathology*, **18**, 535–40.
- Van Buuren, S. and Oudshoorn, C. (2007) *mice: Multivariate Imputation by Chained Equations*. URL <http://web.inter.nl.net/users/S.van.Buuren/mi/html/mice.htm>. R package version 1.16.
- Olesen, K. and Madsen, A. L. (2002) Maximal prime subgraph decomposition of bayesian networks. *IEEE Transactions on Systems, Man, and Cybernetics, Part B*, **32**.
- Osipov, V., Keating, J. T., Faul, P. N., Loda, M. and Dattas, M. W. (2002) Expression of p27 and VHL in renal tumors. *Applied Immunohistochemistry & Molecular Morphology*, **10**, 344–350.
- Roe, J., Kim, H., Lee, S., Kim, S., Cho, E. and Youn, H. (2006) p53 stabilization and transactivation by a von hippel-lindau protein. *Molecular Cell*, **22**, 395–405.
- Strobl, C., Boulesteix, A., Zeileis, A. and Hothorn, T. (2007) Bias in random forest variable importance measures: Illustrations, sources and a solution. *BMC Bioinformatics*, **8**, 25+.
- Tibshirani, R. (1996) Regression shrinkage and selection via the lasso. *J. Royal Statist. Soc.*, **58**, 267–288.
- Wainwright, M., Ravikumar, P. and Lafferty, J. (2007) High-dimensional graphical model selection using ℓ_1 -regularized logistic regression. In *Advances in Neural Information Processing Systems 19* (eds. B. Schölkopf, J. Platt and T. Hoffman), 1465–1472. Cambridge, MA: MIT Press.
- Wenger, R., Stiehl, D. and Camenisch, G. (2005) Integration of oxygen signaling at the consensus hre. *Science Signaling: Signal Transduction Knowledge Environment (STKE)*, **2005**, re12.
- Yuan, M. and Lin, Y. (2006) Model selection and estimation in regression with grouped variables. *Journal of the Royal Statistical Society*, **68**, 49–67.